Vol. 90: 95–115, 2023
https://doi.org/10.3354/cr01719

CLIMATE RESEARCH
Clim Res

Published August 17

Contribution to CR Special 36 'Observed changes in climate over Asia'

Long-term changes in surface air temperature over the Chinese mainland during 1901–2020

Kangmin Wen[1,2,3], Guoyu Ren[1,4,*], Yuyu Ren[4], Lijuan Cao[5], Yun Qin[1,4], Panfeng Zhang[6], Jiajun He[1], Xiaoying Xue[1], Xiubao Sun[7]

[1]Department of Atmospheric Science, School of Environmental Studies, China University of Geosciences (CUG), Wuhan 430074, PR China

[2]Fuzhou Meteorological Bureau, Fuzhou 350028, PR China

[3]Fujian Institute of Meteorological Sciences, Fuzhou 350028, PR China

[4]National Climate Center, China Meteorological Administration (CMA), Beijing 100081, PR China

[5]National Meteorological Information Center, China Meteorological Administration (CMA), Beijing 100081, PR China

[6]School of Tourism and Geographical Sciences, Jilin Normal University, Siping 136000, PR China

[7]State Key Laboratory of Tropical Oceanography, South China Sea Institute of Oceanology, Chinese Academy of Sciences, Guangzhou 510301, PR China

ABSTRACT: The magnitude of long-term surface climate warming over some regions, such as the Chinese mainland, is still uncertain due to the lack of observational data early in the 20th century. In this study, the monthly data series of the average, maximum, and minimum temperatures in the Chinese mainland during 1901–2020 were constructed based on the daily surface air temperature observations from 60 stations across the country, and the characteristics of the average, maximum, and minimum temperature, and diurnal temperature range (DTR) changes were analyzed. Results show that (1) regional average annual mean temperature in the Chinese mainland rose by 0.14°C per decade, maximum temperature rose by 0.07°C per decade, minimum temperature rose by 0.19°C per decade, and DTR decreased by 0.13°C per decade. All these trends are statistically significant ($p < 0.01$); (2) the largest annual mean maximum temperature increase occurred in spring, followed by winter and autumn/summer, and the largest annual mean minimum temperature increase was in winter and spring, followed by autumn and summer; (3) annual mean DTR decreased significantly at a rate of −0.08, −0.12, −0.12, and −0.13°C per decade ($p < 0.01$) in spring, summer, autumn, and winter, respectively; (4) the stations with drops in maximum temperature were mainly in Central China, southern North China, the southeastern coastal areas, and the middle and lower reaches of the Yangtze River, and the stations with significant increases in minimum temperature were located in North China, Northeast China, and Northwest China; (5) the areas with the fastest dropping DTR were mainly located in Northeast China and North China. The maximum and minimum temperature series for China based on climate anomalies are comparable to those based on other currently available datasets.

KEY WORDS: Climate change · Surface air temperature · Diurnal temperature range · Trend · Chinese mainland

1. INTRODUCTION

Global warming over the past century has been confirmed in the global surface temperature record (Jones 2016, Osborn et al. 2021). The Intergovernmental Panel on Climate Change (IPCC) Sixth Assessment Report reported that the global surface temperature was 1.09°C higher in the period of 2011–2020 than in the period of 1850–1900 (IPCC 2021). China is also experiencing rapid warming.

*Corresponding author: guoyoo@cma.gov.cn

Publisher: Inter-Research · www.int-res.com

Over the past century, the annual mean surface temperature in China has increased by approximately 0.5 to 0.8°C (Qin et al. 2007). These long-term changes in the surface temperature have raised widespread concern, and domestic scholars have conducted many studies on climate change during the instrumental period in China (Zhai & Ren 1997, Wang et al. 1998, 2004, Liu et al. 2004, Tang & Ren 2005, Tang et al. 2009, Li et al. 2010, Xu et al. 2011, Cao et al. 2013, 2017, Ding et al. 2014, Zhang 2014, Zhao et al. 2014, Ren et al. 2017, Yang et al. 2017, Wen et al. 2019). These studies have enhanced the understanding of climate change laws in China during the instrumental period and have laid a foundation for understanding the causes and effects of climate change.

Wang et al. (1998) constructed average surface air temperature (SAT) time series for China from 1880 to 2008 based on historical records, ice core records, and tree ring records in western China, referred to here as the WYG series. Tang & Ren (2005) used the mean value of the daily maximum and minimum temperatures from more than 600 stations in China from 1905 to 2001 to calculate a national average temperature series. Tang et al. (2009) made some corrections to the erroneous records existing prior to 1950, performed further quality control, and used 291 stations to develop an average SAT series for China from 1873 to 2008, referred to as the TD series. However, the inhomogeneity of the time series was not considered, and only a limited number of sequences were extended to years prior to 1940. Li et al. (2010) used a 2-stage regression inhomogeneity assessment method to develop a surface temperature series from 1873 to 2004, referred to as the LQX series, in which missing data prior to 1951 were not interpolated. Cao et al. (2013) constructed a set of homogenized monthly mean SAT series for 18 stations in eastern and central China during 1909–2010, referred to as the CLJ series, in which the missing data before 1951 were interpolated. Zhao et al. (2014) found that the regional mean SAT over eastern China exhibited a warming trend of 0.15°C per decade during the period of 1909–2010, using a reconstructed continuous and homogenized SAT series for 16 cities across eastern China. Ren et al. (2017) determined that the change rates in mean temperature, mean maximum temperature, and mean minimum temperature were 0.10, 0.08, and 0.18°C per decade during the period of 1901–2014 in the Hindu Kush Himalayan region, based on LSAT-V1.1 datasets developed by the China Meteorological Administration (CMA). These reconstructed datasets going back to the 19th century cover the whole country or eastern China, but all have a sparse station distribution, and the observational data are scarce during the time before 1950.

Before 1950, especially during the 1940s, the distribution of observational stations in China was very sparse. After that time, observations were rapidly restored and developed. By the end of the 1950s, most of China was covered by high-quality meteorological observations. Although Cao et al. (2017) constructed a new long-term monthly average temperature dataset for the period of 1901 to 2015 in China, based on the homogenized temperature records of 32 stations, there were still fewer early observations than after 1950, and the obtained long-term trends of temperature are likely to be less representative for the whole country. In addition, the long-term changes in maximum and minimum temperature, and diurnal temperature range (DTR) over the last 100 yr or more were not analyzed by Cao et al. (2017).

In this study, we extended the dataset developed by Cao et al. (2017) by adding more early observational stations, and updated the data to 2020. A new homogenized monthly average temperature dataset for the period of 1901 to 2020 with 57 stations covering the whole country was constructed. In addition, we also developed a homogenized monthly maximum and minimum temperature dataset for the same period with 50 stations covering the whole country. Based on the homogenized monthly maximum and minimum temperature dataset, we analyzed the trend characteristics of the maximum and minimum temperatures and DTR in different time periods in China during 1901–2020. This work will improve understanding of the long-term changes in temperature in China, and will also lay a foundation for research into the monitoring, detection, and simulation of regional climate change.

2. MATERIALS AND METHODS

2.1. Data sources

The 'Homogenized monthly temperature dataset of national surface meteorological stations in China (V1.0)' (National Meteorological Information Center [NMIC] 2013a), the 'Homogenized daily temperature dataset of national surface meteorological stations in China (V1.0)' (NMIC 2013b), a 60 station long-sequence temperature dataset for China, and a dataset of the homogenized monthly average tempera-

ture at 32 long-sequence stations in China were all provided by the NMIC of the CMA. The 'Homogenized monthly (daily) temperature dataset of national surface meteorological stations in China (V1.0)' contains the monthly (daily) average temperature and the monthly (daily) average maximum and minimum temperatures at 2419 national stations in China from 1951 to 2020. The monthly dataset was used as a base for the post-1950 data series, and the daily dataset was used to supplement the missed monthly records.

The 60 station long-sequence temperature dataset includes the daily average temperature and the daily average maximum and minimum temperatures, and the sequence lengths are from the beginning of observation to 1950. The time period of the homogenized monthly average temperature dataset from 32 long-sequence stations in China is from 1873 to 2016, and it includes the homogenized monthly average temperature and the average maximum and minimum temperatures (Cao et al. 2017). The 'Homogenized daily temperature dataset of national surface meteorological stations in China (V1.0)' and the 60 station long-sequence temperature dataset were used to construct the preliminary daily and monthly average sequences.

Because the monthly temperature dataset of Cao et al. (2017) contains 32 stations over the whole country, with only 9 stations located to the west of 110° E and a coarser temporal resolution, long-series datasets with additional stations and daily resolution will be urgently needed for studies of extreme temperature change in the country as a whole. On the other hand, the newly digitized daily temperature records from ACRE (Atmospheric Circulation Reconstructions over the Earth) China contains new early data pre-1951, which will contribute to the construction of more accurate long time series for China. In our previous work, the original data and the new data from ACRE China were synthesized to produce a new dataset (Wen 2020). As an example, the newly digitized daily temperature records from ACRE China were used to supplement the missing data for 5 stations (Kunming, Jinan, Lanzhou, Dalian, and Nanning). The data records from ACRE China included January 1929 to April 1938 for Kunming, January 1916 to June 1929 for Jinan, September 1932 to December 1940 for Lanzhou, November 1904 to December 1915 and January 1929 to December 1934 for Dalian, and January 1932 to November 1939 for Nanning. The monthly mean temperatures at these stations were calculated by averaging those of all the days within the months. Compared to the earlier version of the dataset developed by Cao et al. (2017), the new dataset has a much improved coverage of western China, with 15 stations located to the west of 110° E, and a total of 57 stations . Among these 57 stations, 50 have monthly maximum and minimum temperature records. Therefore, the new dataset can provide a better estimate of the early period climatology and long-term trends in SAT in China.

2.2. Merging with earlier data

For the 60 station early temperature data, each station has multiple data sources; therefore, data fusion needed to be carried out. First, the relatively complete data sequence of each station was selected as the basic sequence to be fused. Then, other data from different sources were selected to supplement the missing data according to distance from the observation point of the data. Finally, the early-stage temperature series from each station was sorted as completely as possible, including the file-recorded daily maximum and minimum temperature series. The daily mean temperature series used in this study was calculated according to the arithmetic mean of the file-recorded daily maximum and minimum temperatures.

2.3. Concatenation of data before and after 1950

Since the file numbers of the fully integrated file-recorded daily maximum and minimum temperatures before 1950 were same as those of the 'Homogenized daily temperature dataset of national surface meteorological stations in China (V1.0)' after 1950, we concatenated them by file number. The daily average temperatures calculated via the arithmetic average according to the daily maximum and minimum temperatures were also spliced with the 'Homogenized daily temperature dataset of national surface meteorological stations in China (V1.0)' according to the file number. The period of 1951–1955 corresponds to the time period when the 2 sets of spliced datasets overlap. If both sets of data contained records, the records in the 'Homogenized daily temperature dataset of national surface meteorological stations in China (V1.0)' were selected for 1951–1955 , as these were relatively comprehensive. A monthly average sequence was obtained by calculating the arithmetic average of the daily average sequence.

2.4. Interpolation of missing values

Apart from Hongkong, Macao, Tainan, and Hengchun in Taiwan, a total of 28 stations in mainland China from the monthly average temperature dataset from the 32 long-sequence stations developed by Cao et al. (2017) were used as the underlying dataset, and 29 stations with relatively complete monthly average temperatures were reselected from the 60 long-sequence stations, forming a dataset of up to 57 stations in mainland China. In order to ensure the accuracy and completeness of the data series, the missing data were interpolated by using the records from neighboring stations in the same climate region (Zhang 2014). If there was no record from neighboring stations, the original series remained unchanged. After interpolation, the monthly average temperature dataset was composed of 57 stations (Fig. 1a). For the monthly mean maximum and minimum temperature data, 50 station sequences from the Chinese mainland were selected from the 60 long-sequence stations after being spliced to interpolate missing data; the spatial distribution of these stations is shown in Fig. 1b.

The difference correction method was used to interpolate the missing monthly average temperature, and the average maximum and minimum temperatures (Wen 2020). The interpolation calculation is shown in Eq. (1):

$$p = \frac{\sum_{r=1}^{n}[(X - Y_r + Q_r) \times \mathrm{CORR}_r^2]}{\sum_{r=1}^{n} \mathrm{CORR}_r^2} \quad (1)$$

where p represents the missing value in a certain year and month of the station to be interpolated, X represents the average temperature of the monthly reference period, Q_r represents the average temperature of the reference station in the same year and month, Y_r represents the average temperature of the monthly reference period at the reference station, CORR_r represents the correlation coefficient of the temperature between the station to be interpolated and its corresponding reference station, and n represents the number of reference stations. As a relocation will change all the temperature data in the original temperature series after the relocation year, only the value of the relocation year was changed in the temperature difference sequence; therefore, the missing temperature and the temperature of the relocation year were not considered. The temperature difference sequence of the interpolated station and the temperature difference sequence of its reference stations were used when calculating the corresponding correlation coefficient. The calculation of the difference sequence is shown in Eq. (2):

$$F_i = T_{i+1} - T_i \quad (2)$$

where T_{i+1} represents the temperature value of the $(i + 1)$th year, T_i represents the temperature value of the ith year, and F_i represents the difference value of the ith year. All the temperatures of the overlapping years were included in the calculation, which ensured complete utilization of the data.

The following formula was used to calculate the distance (d) between 2 stations:

$$d(A_1,A_2) = R\cos^{-1}[\sin\varphi_1 \sin\varphi_2 + \cos\varphi_1 \cos\varphi_2 \cos(\theta_1 - \theta_2)] \quad (3)$$

where the latitude and longitude of the city station A_1 are represented by θ_1 and φ_1, respectively, the latitude and longitude of the rural station A_2 are represented by θ_2 and φ_2, respectively, and R is the radius of the Earth, which is 6371 km.

The Yichang station is used as an example to explain the interpolation method for missing temperature values at a station (Zhang 2014). The correlation coefficients are calculated based on the temperature series after 1951 at Yichang station and the 20 sta-

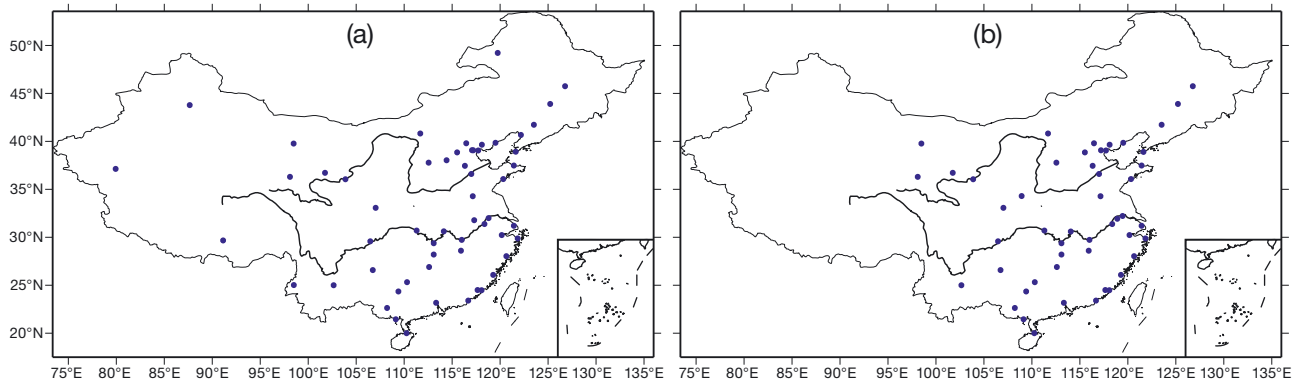

Fig. 1. Distribution of (a) the 57 monthly mean temperature stations and (b) the 50 maximum and minimum temperature stations in the Chinese mainland

Table 1. Starting year, distance from the Yichang station, and correlation coefficient between the annual mean temperatures at 20 stations in the mid-lower Yangtze River valley and the Yichang station

No	Station name	Station no.	Starting year	Correlation coefficient with Yichang	Distance from Yichang (km)
1	Yueyang	57584	1910	0.85	232.6
2	Mapoling	57679	1911	0.79	327.8
3	Wuhan	57494	1887	0.78	287.1
4	Jiujiang	58502	1887	0.77	464.0
5	Anqing	58424	1951	0.76	559.0
6	Hefei	58321	1946	0.74	583.3
7	Wuhu	58334	1934	0.72	689.7
8	Zhenjiang	58248	1947	0.70	795.2
9	Xujiahui	58367	1937	0.70	972.6
10	Nanjing	58238	1907	0.69	730.4
11	Hengyang	57872	1934	0.69	443.1
12	Nanchang	58606	1951	0.67	496.7
13	Hanzhong	57127	1936	0.67	478.3
14	Beilun	58563	1887	0.64	1020.9
15	Hangzhou	58457	1907	0.62	856.2
16	Wenzhou	58659	1887	0.59	958.1
17	Guilin	57957	1936	0.58	612.1
18	Shapingba	57516	1892	0.56	478.4
19	Guiyang	57816	1936	0.48	635.3
20	Fuzhou	58847	1929	0.26	940.0

tions in the same climate region (the middle and lower reaches of the Yangtze River). The starting year of the records at each station and their distance from the Yichang station are given in Table 1.

According to the correlation coefficient of the temperature series between the Yichang station and the other stations in the same climate zone, their distance from the Yichang station, and the parallel observation situation, Yueyang (29.38° N, 113.08° E), Mapoling (28.20° N, 113.08° E), and Wuhan (30.6° N, 114.05° E) were selected as reference stations for the interpolation of the missing values at Yichang. The Yichang station, the reference stations used when interpolating the missing values, the distribution of the other long-sequence stations, and the demarcation of the 6 climatic regions in China are shown in Fig. 2.

Each candidate station and their reference stations contain complete temperature observation records from 1961 to 1990; therefore, these 30 years were taken as the reference period. The missing values at each candidate stations were then interpolated using Eq. (2). The time series of monthly mean temperature before and after interpolation at the Yichang station are shown in Fig. 3. This figure shows that the missing months in the time series of the monthly mean temperature at Yichang occurred in the early 1930s, throughout the 1940s, and in the early 1950s. There were a total of 156 missing months.

2.5. Quality control, inhomogeneity test, and correction

After the interpolation of the early missing data, quality control was performed on the 57 station monthly average temperature dataset and the 50 station monthly average maximum and minimum temperature datasets. The quality control process included the following 3 aspects:

(1) Internal consistency check. The monthly mean minimum temperature should not be greater than the monthly mean maximum temperature. If it is greater, both temperatures in the month are marked as missing values.

(2) Examination of climate extreme values. The monthly average, monthly average maximum, and monthly average minimum temperatures should not exceed 4 SD of the average value of the historical period. If it does, the value is designated as a missing value.

(3) Examination of the climatology limits. The global highest and lowest temperatures reported in the literature (Cerveny et al. 2007) are 57.8 and −89.4°C, respectively. Temperatures should be maintained within the limits of global climatology; therefore, the monthly average, monthly average maximum, and monthly average minimum temperatures should be all within the limit of −89.4 to 57.8°C. If this limit is exceeded, the temperature is regarded as a missing value.

The RHtest V3.0 software (Wang & Feng 2010) was used to check the breakpoints in the monthly se-

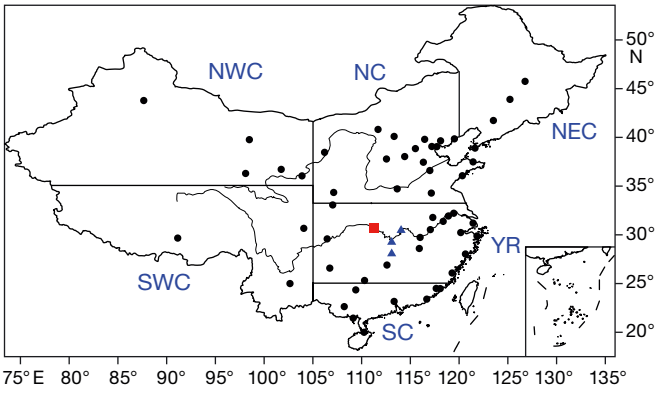

Fig. 2. Selection of reference stations for the interpolation of the missing values at the Yichang station. (■) Yichang station; (▲) 3 reference stations; (●) other long-sequence stations; (black lines) boundaries of the 6 climate zones in China. NWC: Northwest China; NC: North China; NEC: Northeast China; SWC: Southwest China; YR: the mid-lower Yangtze River valley; SC: South China

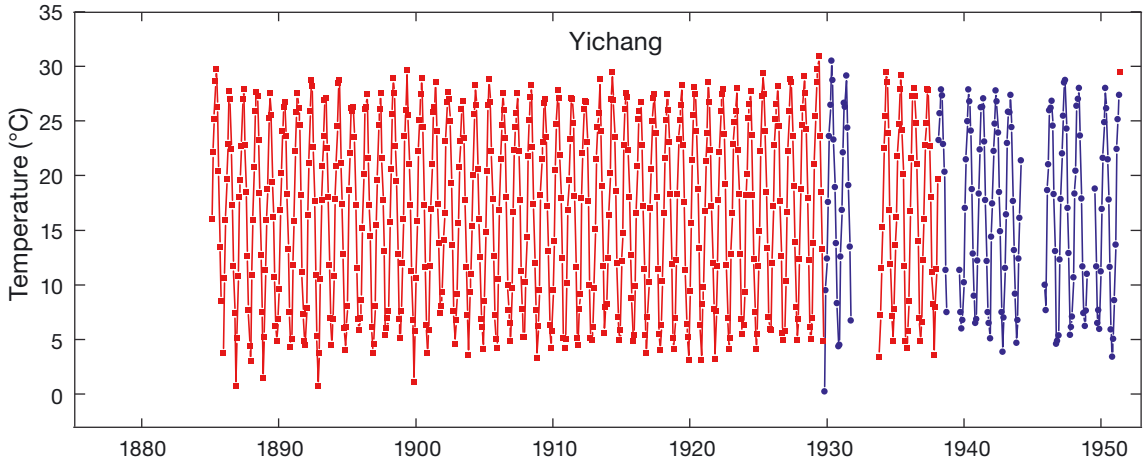

Fig. 3. Time series of the monthly mean temperature (°C) at the Yichang station. Blue lines: interpolated values

quences. This software package includes the PMT and PMF algorithms (Wang 2008a), based on the penalty maximum *t* (PMT) test (Wang 2008a) and the penalty maximum *F* (PMF) test (Wang 2007, 2008b). Both algorithms use recursive testing algorithms to process multiple change points and consider first-order autocorrelation (Wang 2008a). Multiple linear regression algorithms are also embedded in the software; these were used to detect inhomogeneous breakpoints in the monthly and daily sequences. The PMT test is a relatively homogeneous test; therefore, the reference series were used. The PMF test was used without a reference series. Cao & Yan (2012) and Z. Li et al. (2014) found that the PMT algorithm is suitable for the detection of multiple inhomogeneous breakpoints in a dense observation network and that the reference series represents a region. In addition, they found that the PMF algorithm is usually suitable for inhomogeneous breakpoint detection when the observation network is sparse and the reference series is difficult to develop.

In this study, the PMF algorithm was used to detect and correct the inhomogeneous breakpoints in the monthly average temperatures at the 29 added stations and the monthly average maximum and minimum temperatures at all 50 stations. Due to the lack of metadata for the data before 1950, the running Student's *t*-test and the 2-phase regression method (Easterling & Peterson 1995) were also used to improve the accuracy of detecting breakpoints. Only breakpoints found by 2 or 3 algorithms or confirmed by metadata were treated as real change points. When breakpoints found by different methods were adjacent (within 2 years), they were treated as the same one and the occurrence time was confirmed by metadata or set to the first appearing year (Wen 2020). As an example, Fig. 4 shows the time series of the raw and homogenized annual average temperatures at the Yichang station during the period of 1887–2020. Only 1 abrupt change point was found in the monthly mean temperature at Yichang, occurring in January 1922. After correcting this abrupt change point, the annual time series prior to 1922 shifted upward. The homogeneity-adjusted time series obtained in this study for maximum temperature, minimum temperature, and DTR are referred to as T_{maxA}, T_{minA} and DTR_A, respectively.

The annual and seasonal average maximum and minimum temperatures and DTR were analyzed for long-term trends in this study. The DTR was calculated using the maximum and minimum temperatures. The annual and seasonal average temperatures series are presented by Ren et al. (2023, this Special).

2.6. Analysis methods

When establishing the regional average temperature sequence, the Chinese mainland region was divided into 5° × 5° latitude and longitude grids, and the grid area weighting method (Jones & Hulme 1996) was used to obtain the annual temperature series. Winter is defined as December of the previous year to February of the current year, spring is defined as March to May, summer is defined as June to August, autumn is defined as September to November, and the annual temperature is calculated as the arithmetic mean of the 12 months.

China is divided into 6 sub-regions, referring to Xu et al. (2011). These are North China (NC), Northeast

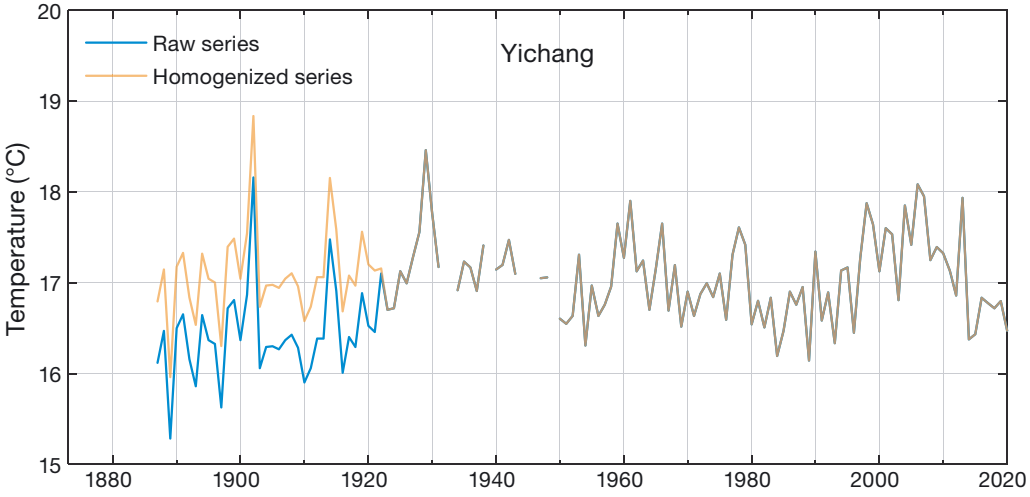

Fig. 4. Time series of the raw and homogenized annual mean temperatures at the Yichang station during the period of 1887–2020. Grey lines: overlap of the two series

China (NEC), Northwest China (NWC), the Yangtze River basin (YR), South China (SC), and Southwest China (SWC). NWC is a sub-region of arid and semi-arid climates, and the main part of the Qinghai-Tibet Plateau is included in SWC. These 2 sub-regions have relatively few stations in terms of their vast areas. The boundaries of the sub-regions are shown in Fig. 2.

The long-term trends of the annual and seasonal mean temperatures were estimated using the Sen-Theil method (Sen 1968, Theil 1992), and the significance of the trends was tested using the Mann-Kendall method (Mann 1945, Kendall 1975). In order to eliminate the autocorrelation effect, we used the nonparametric test. A linear trend was considered statistically significant if it was significant at the 99% ($p < 0.01$) confidence level. The possible influence of serial correlation on the trend estimates was not considered because the data series are long enough (Bayazit & Onoz 2007).

3. RESULTS

3.1. Time series of SAT anomalies

The raw and homogenized annual mean SAT series increased significantly at rates of 1.32 and 1.43°C per decade, respectively, during 1901–2020 ($p < 0.01$). Both data series showed similar features and had a high correlation of 0.99 during 1901–2020, with a weak trend before the late 1960s and a rapid warming after that. Trends of the 2 series for various periods are shown in Table 2. The periods of 1909–2004, 1909–2008, and 1909–1950 were used for the calculations for comparison with previous analyses. For the time period of 1951–2020, the linear trend of the adjusted data (T_{A57}) was 0.21°C per decade, slightly smaller than that of the unadjusted data (T_{UA57}; 0.22°C per decade). These results indicate the complexity of the homogenization effect on the estimated linear trends of SAT. Data homogenization

Table 2. Linear trends of different reconstructed annual mean surface air temperature (SAT) series (°C per decade). –: no value

SAT over China	1909–1950	1909–2004	1909–2008	1901–2015	1951–2015	1901–2020	1951–2020
T_{A57}	0.05	0.14	0.15	0.14	0.20	0.14	0.21
T_{UA57}	0.05	0.12	0.13	0.13	0.22	0.13	0.22
T_{CRU}	0.19	0.07	0.08	0.08	0.16	0.09	0.18
T_{East}	–	–	–	–	0.25	–	0.26
T_{China}	–	–	–	–	0.24	–	0.25
LQX	0.34	0.15	–	–	–	–	–
TD	0.34	–	0.10	–	–	–	–
WYG	0.25	–	0.06	–	–	–	–
CLJ(2013)	0.17	0.14	0.15	–	–	–	–
CLJ(2017)	–	–	–	0.16	0.18	–	–

decreased the upward trend in recent decades, but it increased the positive trends in the earlier period (1909–1950) and the whole period (1901–2020).

To analyze the representativeness of the adjusted data, we also compared the annual mean SAT time series for regions and the whole of China (from all the stations) during 1951–2020 (Fig. 5b). The time series for the whole of China (T_{China}) was calculated by the method of SAT anomaly grid area weighting (Jones & Hulme 1996). The variability of the temperature anomaly approached that of the adjusted data (Fig. 5b), with a correlation coefficient of 0.97 for 1951–2020. Such a high correlation coefficient indicates that the adjusted data provides a good representation of climate change over the whole of China. However, it is also worth noting that the trend of the adjusted data is slightly smaller than that for the whole of China (0.25°C per decade) (Table 2). Moreover, the variation in the adjusted annual mean time series is also in agreement with that of eastern China (to the east of 110° E; termed T_{East}) (Fig. 5b), with a correlation coefficient of 0.98 during 1951–2020.

For the time period 1909–2008, the increasing trend of the adjusted data series was 0.15°C per decade, which is greater than that (0.06–0.10°C) of the 1909–2008 national average series of Wang et al. (1998) and Tang & Ren (2005), but in full accord with that (0.15°C) of the 1909–2008 regional mean series for central and eastern China of Cao et al. (2013). However, the linear trend of the adjusted data

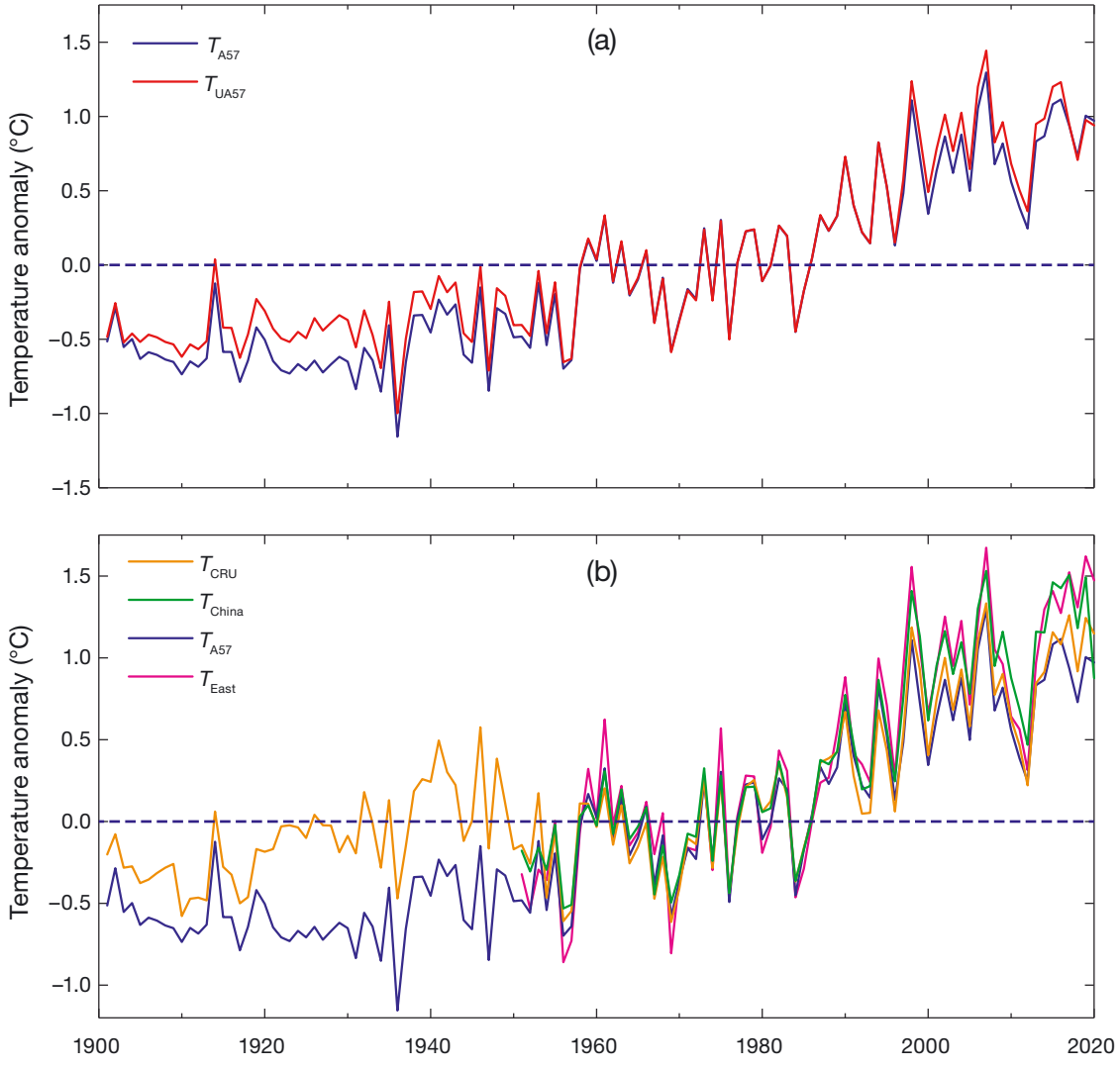

Fig. 5. (a) Time series of the adjusted (T_{A57}) and unadjusted (T_{UA57}) annual mean surface air temperature (SAT) anomalies during 1901–2020. (b) As in (a) but for T_{A57} and the CRU series (T_{CRU}) during 1901–2020, and East China (T_{East}) and the whole of China (T_{China}) during 1951–2020. The reference period is from 1961 to 1990

(0.14°C per decade) during 1909–2004 is slightly smaller than the 0.15°C per decade of LQX (Table 2).

Additionally, we also made a comparison of the adjusted series to the CRU TS v4.06 dataset (Harris et al. 2020). In general, the CRU time series of annual mean temperature anomalies varied consistently with the adjusted temperature data, with a high correlation of up to 0.86 during 1901–2020, though large discrepancies occurred in 1946, 1941, 1937, and 1928, when observations were more sparsely distributed. The linear trend of CRU data was 0.09°C per decade during 1901–2020, smaller than that of the adjusted data, though all these trends are statistically significant ($p < 0.01$).

In following analysis, we focus on the spatial and temporal patterns of long-term change in SAT in China based on the adjusted data.

Fig. 6 shows that the regional maximum temperature increased by 0.07°C per decade ($p < 0.01$). Prior to the end of the 1940s, the maximum temperature increased slowly. From the end of the 1940s to the mid-1980s, it showed a slight downward trend. From the mid-1980s to the end of the 1990s, it increased rapidly. From the end of the 1990s to the present, there was no obvious increase, and the period after 1998 has been termed a warming hiatus (Trenberth & Fasullo 2013, Sun et al. 2017, 2018). The warmest year was 2007, and the coldest year was 1984. The regional minimum temperature increased by 0.19°C per decade, passing the 0.01 significance level. Prior to the mid-1930s, an increase in the minimum temperature was not obvious. From the mid-1930s to the end of the first decade of the 21st century, it increased relatively quickly. Since then, there has not been an obvious increase. The warmest year was 2007, and the coldest year was 1936. The regional DTR decreased by 0.13°C per decade, passing the 0.01 significance level. Prior to the 1950s, a decrease was not obvious; however, since the 1950s, the DTR has decreased rapidly. The largest DTR occurred in 1929, and the smallest occurred in 2012.

3.2. Spatial characteristics of temperature change

As can be seen from Fig. 7a, stations with an average temperature increasing at a rate of 0.20 to 0.44°C per decade were primarily distributed in Northwest, Northeast, South, and North China (Fig. 7d). This may have been partly due to the urbanization effect formed by urban development and global warming (Wen et al. 2019). Among these, the station with the highest rate of temperature increase was in Haikou, with a rate of 0.44°C per decade; the rates at other stations were relatively small, between 0 and 0.20°C per

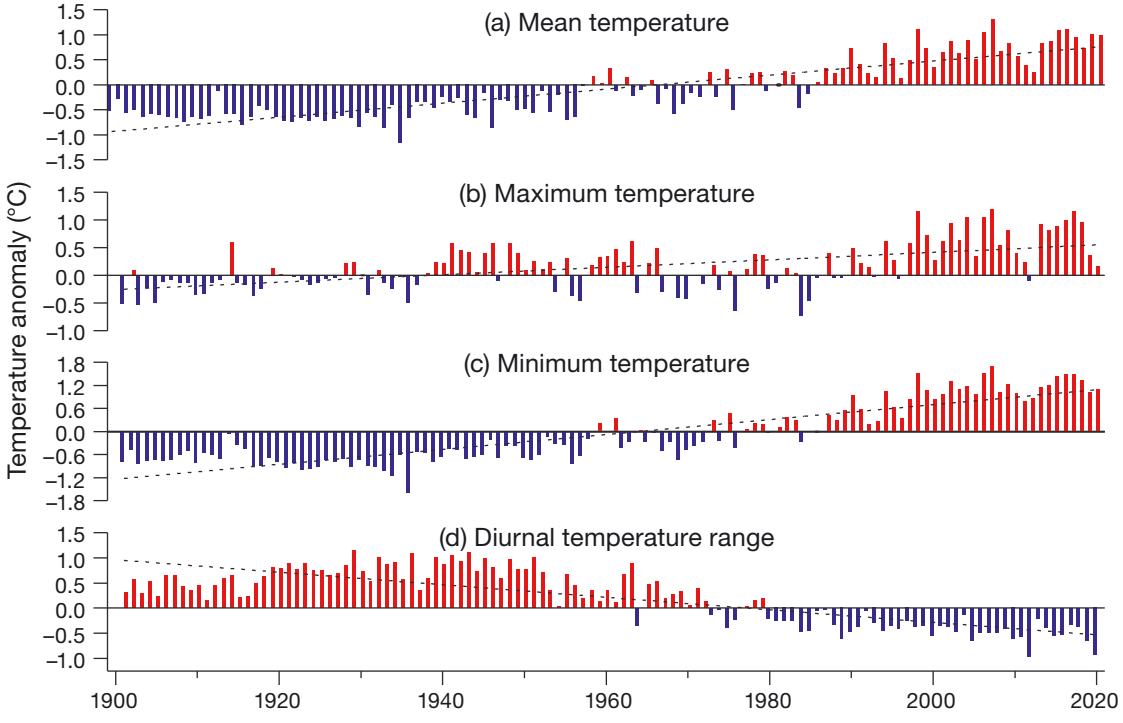

Fig. 6. Annual (a) mean, (b) maximum, and (c) minimum temperatures, and (d) DTR anomalies in the Chinese mainland from 1901–2020 (dashed lines: trend lines). The reference period is the same as in Fig. 5

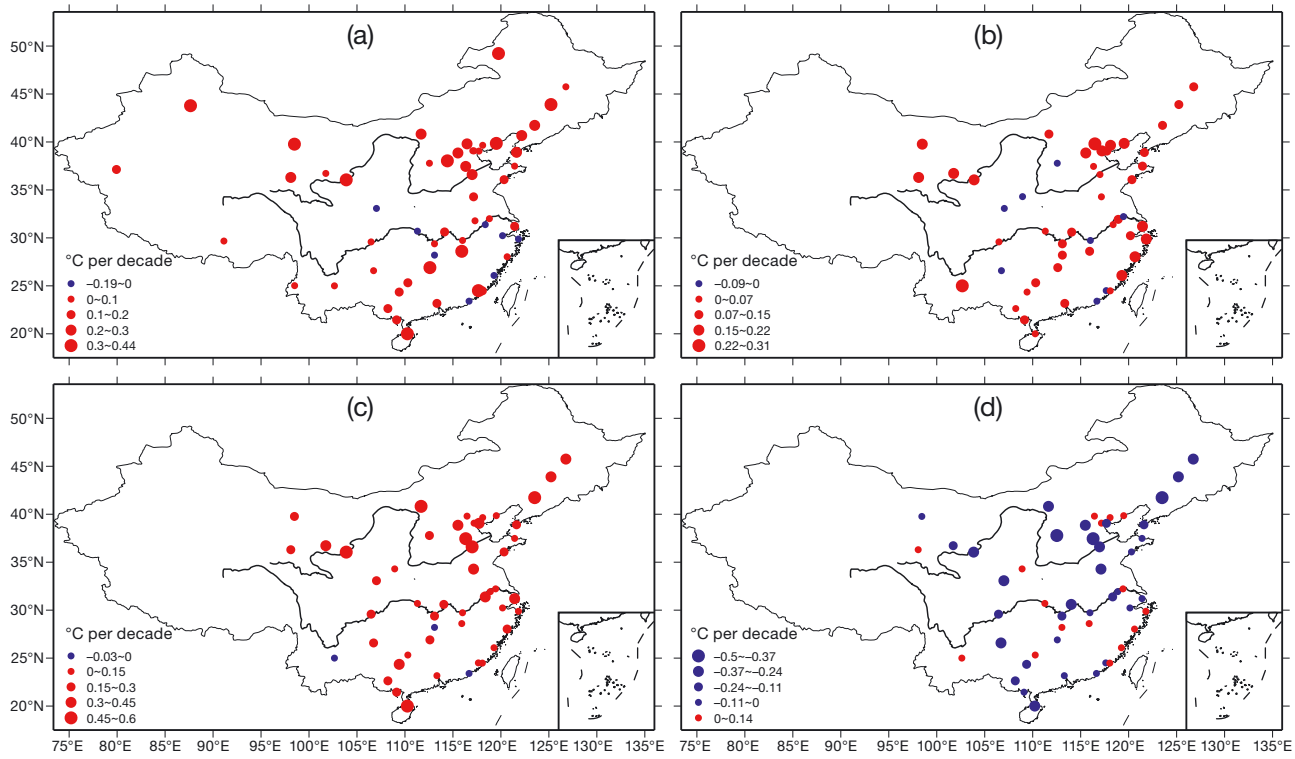

Fig. 7. Spatial distribution of the change trends of the annual (a) mean, (b) maximum, and (c) minimum temperatures, and (d) DTR in the Chinese mainland from 1901–2020. Note that the scales of the circles in different panels are not the same

decade. Stations where the average temperature decreased at a rate from −0.19 to 0°C per decade during 1901–2020 were primarily distributed along the southeastern coast and the middle and lower reaches of the Yangtze River. This may have been partly caused by the urban oasis effect (Wen et al. 2019). Among these, the Fuzhou station had the highest rate of decrease, at −0.19°C per decade. Stations with a maximum temperature increasing at a rate of 0.15 to 0.31°C per decade were primarily distributed in Southwest, Northwest, and North China and in the eastern coastal areas (Fig. 7b). This may have been caused by the urbanization effect formed by urban development and global warming (Wen et al. 2019). Among these, the station with the highest rate of temperature increase was in Kunming, at 0.3°C per decade; the rates of increase at other stations were relatively small, between 0 and 0.15°C per decade. Stations where the maximum temperature decreased at a rate from −0.09 to 0°C per decade during 1901–2020 were primarily distributed in Central and North China, along the southeastern coast, and along the middle and lower reaches of the Yangtze River. This may have been caused by urbanization slowdown, ecological environmental improvement, and partly, by the urban oasis effect formed by urban greening (Wen et al. 2019). Among these, the Zhenjiang station had the highest rate of decrease, at −0.09°C per decade. The rate of increase in minimum temperature was relatively high, with rates of 0.45 to 0.6°C per decade being primarily distributed in North, Northeast, and Northwest China (Fig. 7c). This may have been caused by the urbanization effect formed by urban development and global warming (Wen et al. 2019). Among these, the Dezhou station had the highest rate of increase at 0.6°C per decade. Stations where the minimum temperature decreased at rates from −0.03 to 0°C per decade were primarily distributed in Southwest and South China, and along the middle and lower reaches of the Yangtze River. This may have been caused by the associated atmospheric circulation changes in the context of global warming. Of these, the Kunming station had the highest cooling rate at −0.02°C per decade.

Stations with DTR decreasing at rates from −0.5 to −0.37°C per decade were primarily distributed in Northeast and North China (Fig. 7d). Stations with DTR decreasing at rates from −0.37 to −0.24°C per decade were primarily distributed in Northeast and North China, along the middle and lower reaches of the Yangtze River, and in Central and Northwest China. Stations with an increasing trend in DTR were

primarily distributed along the southeastern coast, along the middle and lower reaches of the Yangtze River, and in North and Central China. Among these, the Mapoling station in Changsha had the largest increasing trend at 0.14°C per decade. The spatiotemporal distribution of DTR has been suggested to be related to cloud cover, solar radiation, elevation, rainfall, and the associated atmospheric circulation changes (Dong & Huang 2015, Xue et al. 2019).

3.3. Time series and spatial characteristics of seasonal temperature

Fig. 8 shows the 4 season mean temperature sequence in China from 1901 to 2020. The regional average temperature in spring increased by 0.18°C per decade, passing the 0.01 significance level. The warmest year was 2018, and the coldest year was 1936. The regional average temperature in summer increased by 0.08°C per decade, passing the 0.01 significance level. The warmest year was 2016, and the coldest year was 1976. The regional average temperature in autumn rose by 0.12°C per decade, passing the 0.01 significance level. The warmest year was 2006, and the coldest year was 1912. The regional average temperature in winter increased by 0.19°C per decade, passing the 0.01 significance level. The warmest year was 1999, and the coldest year was 1936.

Fig. 9 shows the 4 season mean maximum temperature sequence in China from 1901 to 2020. The regional maximum temperature in spring increased by 0.14°C per decade, passing the 0.01 significance level. The warmest year was 2018, and the coldest year was 1936. The regional maximum temperature in summer increased by 0.06°C per decade, passing the 0.01 significance level. The warmest year was 2016, and the coldest year was 1901. The regional maximum temperature in autumn rose by 0.06°C per decade, passing the 0.01 significance level. The warmest year was 1998, and the coldest year was 1981. The regional maximum temperature in winter increased by 0.09°C per decade, passing the 0.01 significance level. The warmest year was 1999, and the coldest year was 1936.

Fig. 10 shows that the regional minimum temperature in spring increased by 0.22°C per decade, passing the 0.01 significance level. Prior to the early 1950s, the minimum temperature increased slowly; from the early 1950s to the mid-1960s, the increase was rapid; and it continued to increase rapidly from the mid-1960s to the present. The warmest year was 2018, and the coldest year was 1936. The regional minimum temperature in summer increased by 0.17°C per decade, passing the 0.01 significance level. From the early 1900s to the early 1910s, it increased rapidly; then was relatively stable until the early 1950s; and increased rapidly from the early 1950s to the early 1960s. From the early 1960s to the mid-1970s,

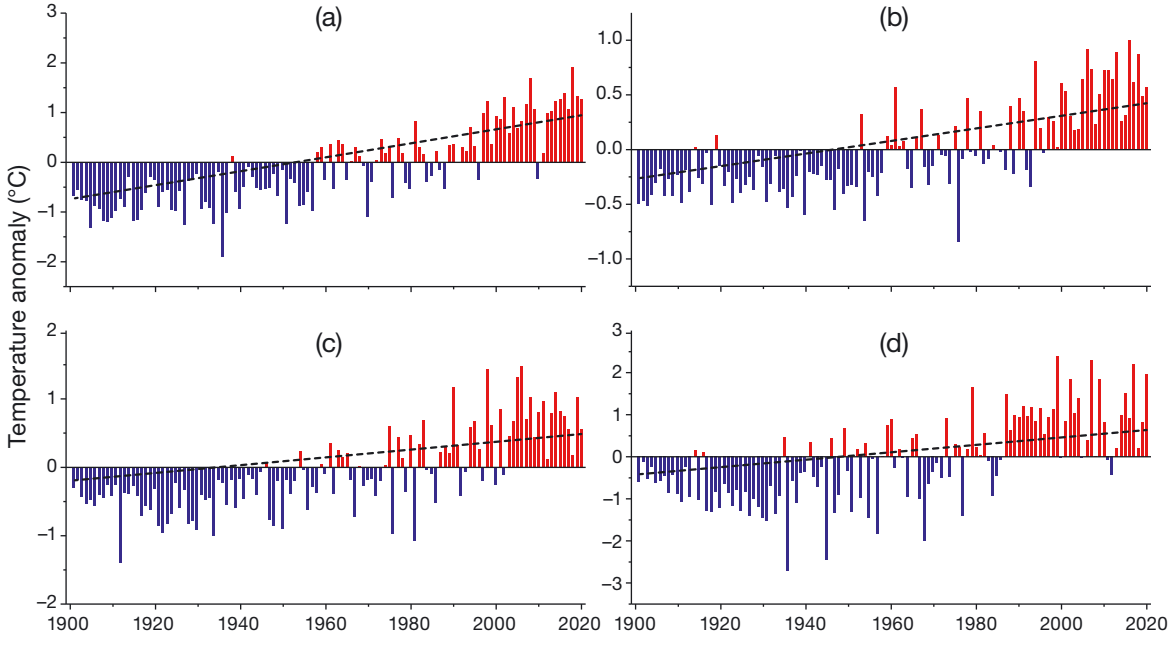

Fig. 8. (a) Spring, (b) summer, (c) autumn, and (d) winter series of annual mean temperature anomalies in the Chinese mainland from 1901–2020 (dashed lines: trend lines). The reference period is the same as in Fig. 5

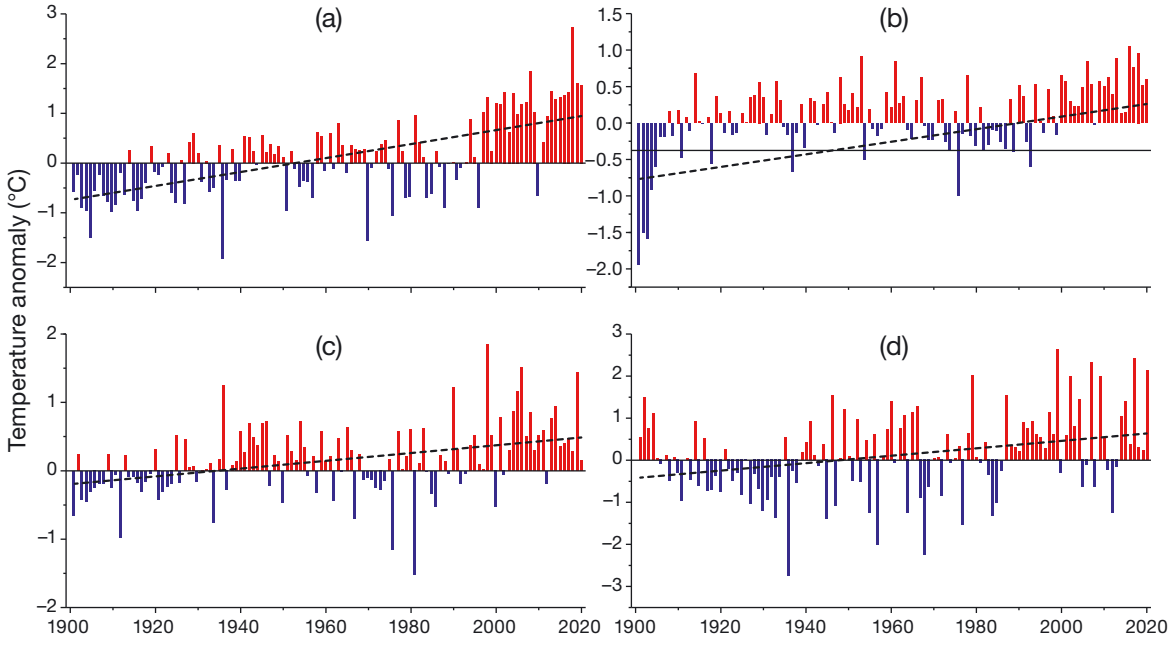

Fig. 9. (a) Spring, (b) summer, (c) autumn, and (d) winter series of seasonal mean maximum temperature anomalies in the Chinese mainland from 1901–2020 (dashed lines: trend lines). The reference period is the same as in Fig. 5

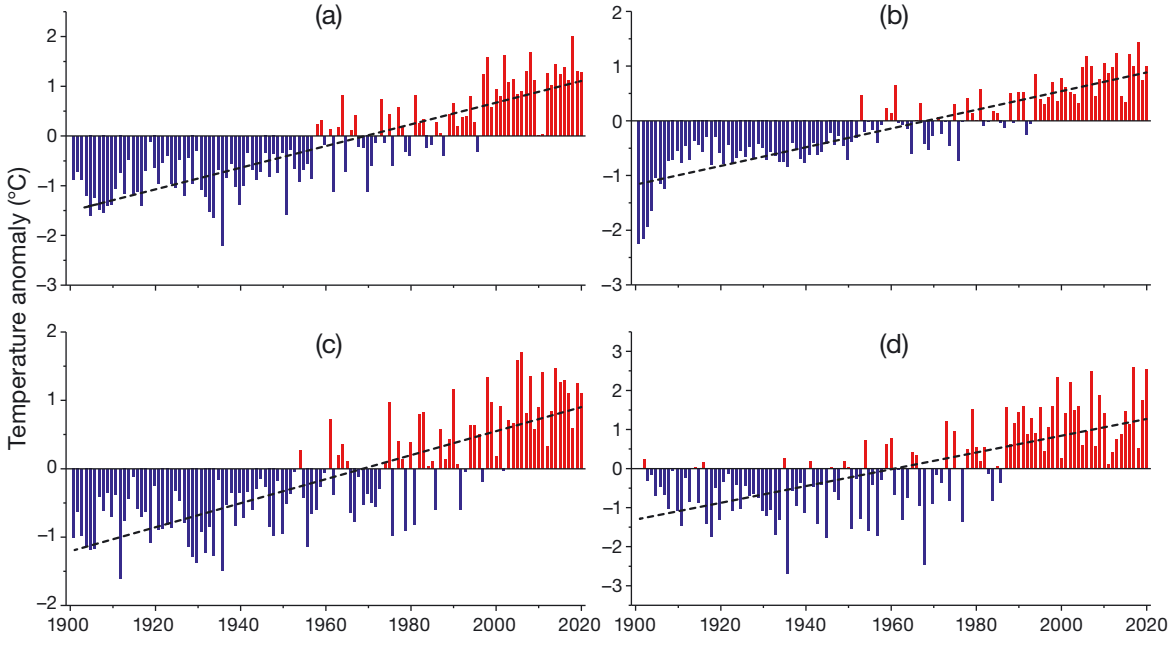

Fig. 10. (a) Spring, (b) summer, (c) autumn, and (d) winter series of seasonal mean minimum temperature anomalies in the Chinese mainland from 1901–2020 (dashed lines: trend lines). The reference period is the same as in Fig. 5

the minimum temperature showed a slight downward trend; and from the mid-1970s to the present, it increased rapidly. The warmest year was 2018, and the coldest year was 1901. The regional minimum temperature in autumn increased by 0.18°C per decade, passing the 0.01 significance level. Prior to the 1950s, there was no obvious increase in minimum temperature. From the 1950s to the early 1960s, the increase became rapid, and it continued to increase rapidly from the early 1960s to the present. The warmest year was 2006, and the coldest year was 1912. The regional minimum temperature in winter

increased by 0.22°C per decade, passing the 0.01 significance level. Prior to the end of the 1950s, the minimum temperature increased slowly. In the 1960s, it showed a decreasing trend. From the end of the 1960s to the present, it increased rapidly. The warmest year was 2017, and the coldest year was 1936.

The DTR during the 4 seasons in China from 1901 to 2020 showed a weakly increasing stage prior to the 1930s, a weakly decreasing stage from the early 1930s to the early 1950s, and a rapidly decreasing stage from the early 1950s to the present (Fig. 11). The regional spring DTR decreased by approximately 0.08°C per decade, passing the 0.01 significance level. Prior to the 1930s, it showed a slight upward trend, while from the 1930s to the early 1950s, it showed a slow downward trend. From the early 1950s to the present, the DTR decreased rapidly. The largest anomaly occurred in 1929, and the smallest anomaly occurred in 2010. The regional summer DTR decreased by 0.12°C per decade, passing the 0.01 significance level. Prior to the 1930s, the DTR showed a slight upward trend, and from the 1930s to the end of the 1940s, it showed a slight downward trend. Since then, it has shown a rapid downward trend. The largest anomaly year was 1933, and the smallest anomaly year was 1998. The regional autumn DTR decreased by 0.12°C per decade, passing the 0.01 significance level. Prior to the end of the 1930s, the DTR showed an upward trend; then, until the early 1950s, it showed a slight downward trend. From the early 1950s to the present, it decreased rapidly. The largest anomaly occurred in 1936, and the smallest anomaly occurred in 2020. The regional winter DTR decreased by 0.13°C per decade, passing the 0.01 significance level. Prior to the mid-1930s, the DTR was relatively stable; from the early 1940s to the early 1950s, it showed a slow downward trend; and after the early 1950s, the downward trend was relatively rapid. The largest anomaly occurred in 1963, and the smallest anomaly occurred in 2012.

For the average temperature in spring, only Yichang and Fuzhou stations, which are located in Central and Southeast China, showed cooling trends. Stations with higher rates of increase were primarily located along the middle and lower reaches of the Yangtze River, in North, South, Northwest, and Northeast China, and the Tibet Plateau. In summer, most stations showed warming trends, but the number of stations with cooling trends increased compared to spring. Stations with higher rates of increase were primarily located in Northwest, South, and North China. Stations with decreasing trends were primarily distributed in Southwest China and along the middle and lower reaches of the Yangtze River. In autumn, most stations also showed warming trends. Stations with higher rates of increase were primarily distributed in North, Northwest, Northeast, and South China, and the Tibet Plateau, and the stations with decreasing trends were primarily distributed in Southeast China, along the middle and lower

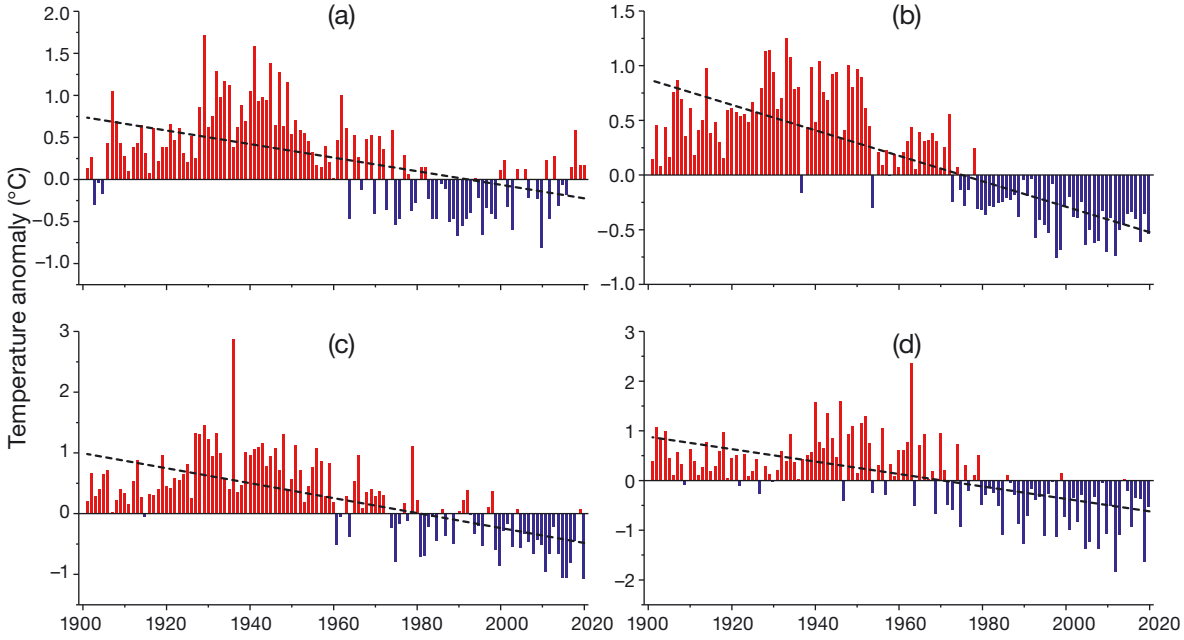

Fig. 11. (a) Spring, (b) summer, (c) autumn, and (d) winter series of seasonal mean DTR anomalies from 1901–2020 in the Chinese mainland (dashed lines: trend lines). The reference period is the same as in Fig. 5

reaches of the Yangtze River. In winter, the stations with higher rates of increase were primarily distributed in North, Northeast, South, and Northwest China, and the Tibet Plateau, and stations with decreasing trends were generally located in Southwest, Southeast, and Central China (data not shown).

For the maximum average temperature in spring, most stations showed warming trends. Stations with higher rates of increase rate were primarily located along the southeastern coast and in North and Central China, while stations with decreasing trends were mostly located in Southwest, Northwest, and North China. In summer, most stations showed warming trends, but the number of stations with cooling trends increased compared to spring. Stations with higher rates of increase were primarily located in Southwest China, along the southeastern coast, and in North China. Stations with decreasing trends were primarily distributed in North and Northwest China, along the middle and lower reaches of the Yangtze River, and in Southwest China. This may relate to urbanization slowdown, ecological environmental improvement, and partly, by the urban oasis effect formed by urban greening (Wen et al. 2019). In autumn, most stations also showed warming trends. Stations with higher rates of increase were primarily distributed in North, Northwest, and Southwest China, and along the southeastern coastal areas, and the stations with decreasing trends were primarily distributed in North, Northwest, and Southwest China, along the middle and lower reaches of the Yangtze River, and in South China. In winter, the stations with higher rates of increase were primarily distributed in North and Northwest China, along the middle and lower reaches of the Yangtze River, and in the southeastern coastal areas, and stations with decreasing trends were generally located along the middle and lower reaches of the Yangtze River (data not shown).

For the minimum average temperature in spring, a decreasing trend only occurred in Kunming, while other stations all showed warming trends. Those with higher rates of increase were primarily located in Northeast and North China, and in Hainan. In summer, stations with higher rates of increase were primarily located in Northeast and North China, and in Hainan, and stations with decreasing trends were only distributed in Northwest China and along the middle and lower reaches of the Yangtze River. In autumn, warming was also a dominant feature in most areas. Stations with higher rates of increase were primarily located in Northeast, North, and Northwest China, along the lower reaches of the Yangtze River, and in Hainan, and stations with downward trends appeared in Southwest and Central China, and along the southeastern coastal areas. In winter, warming was the dominant feature in most areas, and the warming trend was more obvious than in other seasons. Stations with higher rates of increase were primarily located in Northeast, North, and Northwest China, along the middle and lower reaches of the Yangtze River, and in Hainan, and the stations with decreasing trends occurred in the southwestern and southeastern coastal areas (data not shown).

The seasonal mean DTR exhibited a general downward trend across the country. In spring, stations with higher rates of decrease were primarily located in North and Northeast China, and stations with slight increasing trends occurred in North and Central China, along the middle and lower reaches of the Yangtze River, and in southwestern and southeastern coastal areas. In summer, the number of stations with a decreasing trend increased compared to spring. Stations with larger decreasing trends were primarily located in North and Northeast China, and along the middle and lower reaches of the Yangtze River, and the stations with slight increasing trends were located along the lower reaches of the Yangtze River and in Central, North, and Southwest China. In autumn, the number of stations with decreasing trends was highest. Stations with larger decreasing trends were mostly located in North and Northeast China, and stations with slight increasing trends were only distributed along the middle and lower reaches of the Yangtze River, and in the southwestern and eastern coastal areas. In winter, stations with larger decreasing trends were also primarily located in North and Northeast China, and stations with weak increasing trends occurred in Central China, eastern coastal areas, Southwest China, and some coastal areas of South China (data not shown).

3.4. Time series of regional average temperature

The average, maximum, and minimum temperature, and DTR trends for 6 climate zones and the Chinese mainland as a whole during 1901–2020 are shown in Table 3. The annual average temperatures of the zones all presented warming trends. The smallest increasing trend appeared in the Yangtze River region, with a rate of 0.02°C per decade, and the highest warming trends appeared in Northeast, Northwest, and North China, with rates of 0.27, 0.25, and 0.21°C per decade, respectively. The annual mean maximum temperatures of the zones all presented warming trends. The smallest increasing

trend appeared in the Yangtze River region, with a rate of 0.04°C per decade, and the largest warming trends appeared in Southwest, Northwest, and North China, with rates of 0.29, 0.21, and 0.15°C per decade, respectively. The annual mean minimum temperatures of the regions all exhibited warming trends except for Southwest China, which showed a weak cooling trend, with a rate of −0.02°C per decade. The smallest increasing trend appeared in the Yangtze River region and South China, with a rate of 0.12°C per decade, and the largest warming trends appeared in Northeast, Northwest, and North China, with rates of 0.38, 0.37, and 0.35°C per decade, respectively. The annual mean DTR of the regions all exhibited downward trends except for Southwest China, which showed a weak increase, with a rate of 0.05°C per decade. The smallest negative trends appeared in South China and the Yangtze River region (−0.05 and −0.08°C per decade), and the largest negative trends appeared in Northeast, North, and Northwest China, with rates reaching −0.29, −0.26, and −0.18°C per decade, respectively.

Seasonal average temperature also exhibited warming trends in all zones except the Yangtze River region in summer. The least warming in spring occurred in the Yangtze River. The Yangtze River showed a slight chilling at a rate of −0.01°C per decade in summer, but Northeast, Northwest, and North China all experienced evident warming. The smallest autumn mean SAT warming appeared in the Yangtze River, and the largest appeared in Northwest China. The smallest winter warming occurred in the Yangtze River, and the largest value was recorded in Northeast China. For Northeast and Northwest China, the winter witnessed the highest increases in average temperature among the 4 seasons. Seasonal mean maximum temperature also exhibited warming trends in all zones except Northeast China in summer. The smallest warming in spring was recorded in the Yangtze River. Northeast China showed a slight chilling at a rate of −0.05°C per decade in summer, but Southwest and Northwest China experienced obvious warming. The smallest warming in autumn appeared in the Yangtze River, and the largest trend appeared in Southwest China. The least warming in winter occurred in South China and the Yangtze River, and the largest value occurred in Southwest China. For Northeast, North, and Northwest China, the winter witnessed the highest increases in maximum temperature among the 4 seasons. Seasonal mean minimum temperature exhibited warming trends in all zones except in spring, autumn, and winter in Southwest China. For spring, Southwest China showed a slight cooling at a rate of −0.02°C per decade, the smallest spring warming was seen in the Yangtze River. For summer, the least warming was seen in Southwest China. Autumn in Southwest China showed a trend of 0, and the least warming occurred in the Yangtze River and South China. In winter, Southwest China showed a slight cooling at a rate of −0.11°C per decade, and the least winter warming was recorded in South China. For Northeast, North, and Northwest China, the winter showed the largest increases in minimum temperature among the 4 seasons.

Seasonal mean DTR showed decreasing trends in all regions except in Southwest China during all seasons. The largest spring decrease was recorded in Northeast China. In summer, the largest decrease was also seen in Northeast China. The largest autumn downward trends were seen in Northeast and North China, with rates reaching −0.29°C per decade. For winter, the greatest decrease was seen in Northwest China. In Northwest China and the Chinese mainland as a whole, the winter showed the largest decreases in DTR among the 4 seasons.

In conclusion, the regions of North, Northeast, and Northwest China exhibited more obvious warming in average temperatures and minimum temperatures, and more obvious declines in DTR than other regions. The DTR declines in these regions may mostly be due to the increased minimum temperatures. The regions of North and Northwest China exhibited more obvious warming in maximum and minimum temperatures than other regions. Southwest China experienced more obvious warming in maximum temperature than other regions, but not in minimum temperature. The region of Northeast China exhibited more obvious warming in minimum temperature than other regions, but not in maximum temperature. North and Northeast China presented the largest and most obvious decreases in DTR in all seasons. The Yangtze River and South China showed the smallest decreases in DTR in all 4 seasons. The trends of annual and seasonal average, mean maximum and minimum temperatures, and DTR were significant in all regions except for the summer maximum temperature for the Yangtze River, summer minimum temperature in Southwest China and the Yangtze River, autumn minimum temperature in Southwest China, and spring DTR in Southwest China.

4. DISCUSSION

In order to compare with previous studies, we constructed a nationally averaged SAT anomaly series,

including raw and homogenized average SAT anomaly series (anomalies are relative to the 1901–2000 annual means). The raw and homogenized data series have an increase rate of 0.20 and 0.22°C per decade during 1901–2020, respectively (Table 4), with the homogenized data series seeing a slight larger trend.

A previous analysis (Li & Yang 2019) assumed that the lack of data early in the 20th century, especially for western China may have been the reason for the abnormally warm anomalies in 1940s reported by Tang & Ren (2005) and Soon et al. (2015, 2018). In this study, we added new digitalized data for the pre-1950 period from western stations, which should make the nationally averaged SAT series more reliable, especially for the early 20th century (1920s to 1940s) warm periods in China.

We compared the anomalies and trends of different periods in the raw and homogenized data series, and our homogenized series with the analysis by Soon et al. (2018). The recent warm peak year (2007) during 1951–2020 was 1.45°C warmer than the early 20th century (1901–1950) warm peak year (1946) in the homogenized data series. According to the difference (ΔT) between these 2 peak years (1.45°C), the early warm peak year in our homogenized series ranks last in the table published by Soon et al. (2018; their Table 1). The linear trends for the early (1901–1950) and late (1951–2000) 20th century in our homogenized series were 0.32 and 0.19°C per decade, respectively, and the temperatures of the warmest years (1946 and 2007) during the same periods were 1.19 and 2.64°C above average, respectively. The trend during 1901–2000 was 0.22°C per decade, and the difference between the trends for 1901–1950 and 1951–2000 was –0.13°C per decade. Our data series identified the same year (1946) as the warmest year in the 1901–1950 period, which is consistent with the results of Soon et al. (2015, 2018). Our 2 series also identified the same year (2007) as the warmest year in the 1951–2020 period, and this is consistent with the results of most previous analyses, though there are studies that indicate 1998 as the warmest for the 1951–present period.

Table 3. Trends of annual (Ann) and seasonal (Spr: spring; Sum: summer; Aut: autumn; Win: winter) average (T_{ave}), maximum (T_{max}), and minimum temperature (T_{min}), and diurnal temperature range (DTR) for 6 climate regions in the Chinese mainland during 1901–2020 (°C per decade). See Fig. 2 for definition of zone abbreviations. *$p < 0.05$

Region	T_{ave}					T_{max}					T_{min}					DTR				
	Ann	Spr	Sum	Aut	Win	Ann	Spr	Sum	Aut	Win	Ann	Spr	Sum	Aut	Win	Ann	Spr	Sum	Aut	Win
Chinese mainland	0.14*	0.18*	0.08*	0.12*	0.19*	0.07*	0.14*	0.06*	0.06*	0.09*	0.19*	0.22*	0.17*	0.18*	0.22*	–0.13*	–0.08*	–0.12*	–0.12*	–0.13*
NEC	0.27*	0.35*	0.14*	0.22*	0.39*	0.09*	0.18*	–0.05*	0.05*	0.19*	0.38*	0.44*	0.28*	0.33*	0.46*	–0.29*	–0.26*	–0.32*	–0.29*	–0.31*
NC	0.21*	0.26*	0.14*	0.16*	0.26*	0.15*	0.22*	0.04*	0.09*	0.24*	0.35*	0.4*	0.27*	0.33*	0.42*	–0.26*	–0.24*	–0.25*	–0.29*	–0.26*
NWC	0.25*	0.25*	0.15*	0.25*	0.36*	0.21*	0.21*	0.18*	0.21*	0.23*	0.37*	0.34*	0.2*	0.37*	0.57*	–0.18*	–0.16*	–0.05*	–0.18*	–0.34*
SWC	0.12*	0.12*	0.07*	0.15*	0.15*	0.29*	0.25*	0.33*	0.34*	0.25*	–0.02*	–0.02*	0.05	0	–0.11*	0.05*	0.003	0.02*	0.07*	0.09*
YR	0.02*	0.06*	–0.01*	0.01*	0.04*	0.04*	0.1*	0.005	0.02*	0.05*	0.12*	0.14*	0.1	0.11*	0.14*	–0.08*	–0.04*	–0.1*	–0.1*	–0.09*
SC	0.13*	0.16*	0.12*	0.12*	0.12*	0.06*	0.12*	0.06*	0.03*	0.05*	0.12*	0.15*	0.11*	0.11*	0.11*	–0.05*	–0.02*	–0.05*	–0.08*	–0.06*

Table 4. Linear trends for the early (1901–1950) and late (1951–2000) 20th century, along with the temperature anomalies of the hottest years during the 1901–1950 and 1951–2020 periods, for both of the raw and homogenized series. Temperature anomalies (°C) are departures relative to the 1901–2000 means

	Period	1901–2020 Trend (°C per decade)	1901–2000 Trend (°C per decade)	1901–1950 Trend (°C per decade)	1901–1950 Peak T (°C)	1901–1950 Peak year	1951–2000 Trend (°C per decade)	1951–2020 Peak T (°C)	1951–2020 Peak year	Differences Δ Trend (°C per decade)	Differences ΔT (°C)
Raw series	1901–2020	0.20	0.20	0.32	1.24	1946	0.19	2.70	2007	–0.13	1.45
Homogenized series	1901–2020	0.22	0.22	0.32	1.19	1946	0.19	2.64	2007	–0.13	1.45

Our homogenized data series suggests that the recent warm peak year (2007) was warmer than the earlier peak year (1946). This is approximately consistent with Wang et al. (2004), Tang & Ren (2005), Ding et al. (2014), the raw series, and the series of Li et al. (2017). However, our series suggests a higher warming rate for the 1901–1950 period (0.32°C per decade) than for the 1951–2000 period (0.19°C per decade). This is consistent with the results of Soon et al. (2015, 2018).

The peak year temperature anomaly of the raw series was 1.24°C during 1901–1950, but it decreased to 1.19°C after data homogenization. The specific reasons for this remain to be studied in the future. In addition, both the homogenized and raw series were homogenized after 1951, because the data for years after 1951 were acquired directly from the NMIC and had already been homogenized. Therefore, the peak year temperature anomalies of the raw series and the homogenized series during 1951–2020 were almost the same. Because the 57 stations used to construct the present series are mostly located in cities, the relative warmth of the recent period in our 2 series is very consistent with that of the GHCN v4 (raw) data (Soon et al. 2018), which was constructed based on a dataset obtained mostly from urban stations.

Sun et al. (2019) studied the global DTR change from 1901 to 2014 and found that the global and hemispheric DTR decreased by 0.35 and 0.42°C, respectively, from 1951 to 2014. From 1901 to 2014, they decreased by 0.41 and 0.42°C. They also found the DTR over China decreased by 1.15°C during 1951–2014 and by 1.37°C during 1901–2014 (Sun et al. 2019); both decreases were larger than those of the global and hemispheric ranges (Table 5). This difference is primarily due to the different study ranges: China is a developing country with rapid urbanization and a significant rise in minimum temperature, which has led to a significant decline in DTR. Sun et al. (2021) studied the DTR in East Asia during 1901–2018 and showed that the DTR decreased by 0.53°C during 1951–2018 and by 0.6°C during 1901–2018. The DTR in China decreased by 1.16°C during 1951–2018 and by 1.42°C during 1901–2018 in the present study (Table 5). These decreases in the DTR were both larger than those in East Asia as a result of the different areas studied. Easterling et al. (1997) analyzed the change trend of the maximum and minimum temperatures in the Northern Hemisphere from 1950 to 1993 and found that they increased by 0.09 and 0.18°C per decade, respectively. Over the same period, the maximum temperature decreased by 0.03°C per decade over China in our study, which is slightly lower than the overall decrease in the Northern Hemisphere. The minimum temperature increased by 0.21°C per decade, close to the trend calculated for the Northern Hemisphere (Table 5). In addition, when analyzing global climate change, some scholars (Wang & Ye 1995, Wang 2001, Wang et al. 2014) have identified a warming acceleration period from 1979 to 1999; this is in agreement with the warming acceleration period found in the time series of the maximum and minimum temperatures in our study.

Karl et al. (1991, 1993) concluded that the DTR in China during 1951–1988 and 1951–1989 both de-

Table 5. Linear trends of different reconstructed diurnal temperature range (DTR), maximum temperature (T_{max}), and minimum temperature (T_{min}) series (°C per decade). The homogeneity adjusted time series obtained in this paper are referred to as T_{maxA}, T_{minA} and DTR_A, respectively

Period	Reference	DTR					T_{max}			T_{min}		
		Global	Northern Hemisphere	East Asia	China	China DTR_A	Northern Hemisphere	China	China T_{maxA}	Northern Hemisphere	China	China T_{minA}
1951–2014	Sun et al. (2019)	−0.05	−0.07			−0.18						
1901–2014	Sun et al. (2019)	−0.04	−0.04			−0.12						
1951–2018	Sun et al. (2021)			−0.08		−0.09						
1901–2018	Sun et al. (2021)			−0.05		−0.12						
1950–1993	Easterling et al. (1997)						0.09		−0.03	0.18		0.21
1951–1988	Karl et al. (1991)				−0.2	−0.25						
1951–1989	Karl et al. (1993)				−0.2	−0.26						
1950–1999	Shen & Varis (2001)				−0.24	−0.23						
1955–2000	Liu et al. (2004)				−0.2	−0.22		0.13	0.07		0.32	0.26
1955–1989	Liu et al. (2004)				−0.25	−0.26		−0.02	−0.07		0.24	0.19
1990–2000	Liu et al. (2004)				0.05	−0.11		0.56	0.42		0.51	0.33
1951–1990	Zhai & Ren (1997)				−0.13	−0.26		0.03	−0.04		0.18	0.21
1951–2002	Tang et al. (2005)				−0.17	−0.21		0.12	0.08		0.28	0.27

creased by 0.2°C per decade. During the same periods, the DTR over China decreased by 0.25 and 0.26°C per decade, respectively; this is slightly larger than the previously obtained decreasing trend (Table 5). This may be due to inconsistency of the study data. Shen & Varis (2001) analyzed the DTR changes from 1950 to 1999 in China with data from 400 stations and found that it decreased at a rate of −0.24°C per decade. The DTR in China decreased at a rate of −0.23°C per decade from 1950 to 1999 in our study. This is in good agreement with the previous results and helps verify the accuracy of the results of this study. Liu et al. (2004) analyzed the average, maximum, and minimum temperatures, and DTR in China from 1955 to 2000 and found that the maximum and minimum temperatures increased by 0.13 and 0.32°C per decade, respectively, while the DTR decreased by 0.2°C per decade. During 1955–1989, they found that the maximum temperature decreased by 0.02°C per decade, the minimum temperature increased by 0.24°C per decade, and the DTR decreased by 0.25°C per decade. During 1990–2000, they found that the maximum and minimum temperatures increased by 0.56 and 0.51°C per decade, and the DTR increased by 0.05°C per decade. During 1955–2000, the maximum and minimum temperatures in China increased by 0.07 and 0.26°C per decade, respectively, both of which are slightly smaller than the previous results, and the DTR decreased by 0.22°C per decade, which is very close to the previous result. During the period of 1955–1989, the maximum temperature decreased by 0.07°C per decade and the minimum temperature increased by 0.19°C per decade, both of which are slightly smaller than the previous results, and the DTR decreased by 0.26°C per decade, which is very close to the previous result. During the period of 1990–2000, the maximum and minimum temperatures increased by 0.42 and 0.33°C per decade, and the DTR decreased by 0.11°C per decade; these values are slightly smaller than the previous results (Table 5). This is primarily due to the use of different stations.

Zhai & Ren (1997) used data from 369 observation stations compiled by the NMIC to study the maximum and minimum temperatures, and DTR in China from 1951 to 1990. They found that the maximum and minimum temperatures increased by 0.03 and 0.18°C per decade, and the DTR decreased by 0.13°C per decade. We recalculated the maximum and minimum temperatures, and DTR trends in China during the period from 1951 to 1990 and found that the maximum temperature decreased by 0.04°C per decade, which is slightly lower than the previous result, and that the minimum temperature increased by 0.21°C per decade, which is only slightly higher than the previous result. The DTR decreased by 0.26°C per decade, which is higher than the previous result (Table 5). The slight differences in the maximum and minimum temperatures are primarily caused by the different station data used. The differences in DTR are largely a consequence of the fact that the 50 stations used in our study are almost all located in cities. The larger increase in minimum temperature is due to urbanization development after 1951, which caused a more obvious decline in the DTR. In addition, urbanization and relocation factors played a role in creating differences. Tang et al. (2005) analyzed the changes in the average maximum and minimum temperatures and the DTR in China from 1951 to 2002 and found that the maximum and minimum temperatures increased by 0.12 and 0.28°C per decade, respectively, and the DTR decreased by 0.17°C per decade. We recalculated the trend during the same period and found that the maximum and minimum temperatures increased by 0.08 and 0.27°C per decade, and the DTR decreased by 0.21°C per decade, all of which are relatively close to the results of the previous analysis, showing the accuracy of our results (Table 5).

The direct cause for the change in the DTR is the different changes in the daily maximum surface air temperature (SAT_{max}) and minimum surface air temperature (SAT_{min}) (Easterling et al. 2000, IPCC 2013, Sun et al. 2019, Yang et al. 2022). In addition to the direct influences of solar radiation on the intra seasonal changes in SAT_{max} and SAT_{min}, the changes in land use/land cover (LULC) and the intra seasonal change in land surface thermal conditions significantly affect the atmospheric thermal conditions at the observation stations. Yang et al. (2020) showed a significant composite effect of agricultural activities and urbanization on the daytime–nighttime difference in land surface temperature (LST) and DTR, and their regional differences. For example, they discovered that the change in the DTR in the NYRD (North of Yangtze River Delta) area is largely attributable to nighttime temperature (nighttime LST) and SAT_{min}. The land cover changes caused by crop rotation influence the nighttime LST and SAT_{min}. However, the national weather stations are usually located in or near cities or towns in China, and the SAT records are heavily influenced by local human activities, especially the urbanization process (Ren & Ren 2011, J. Yang et al. 2013, Y. Yang et al. 2013, Yang et al. 2017, Wang et al. 2019). Previous research has shown that the long-term downward trend of DTR has been significantly affected by urbanization

in China, in particular in North China (Zhou & Ren 2011, Ren et al. 2015). The changes in annual mean DTR in different regions of China are also related to altitude, cloudiness, precipitation, soil moisture, and other factors (Hua et al. 2006, Chen & Chen 2007, Dong & Huang 2015, Sun et al. 2021). The specific reasons for the regional differences in DTR and its trends should be further explored in the future.

It should be noted that using homogenized data corrected for inhomogeneity breakpoints caused by relocations from urban areas to suburban areas may have caused a new system bias due to urbanization (J. Li et al. 2014, Zhang et al. 2014, Ren et al. 2015, Bian et al. 2017), resulting in a greater urbanization effect in the data series after the adjustment. This may have been a major reason for the larger upward trends in annual mean temperature being estimated from the homogenized data than from unadjusted data since the beginning of the 20th century in China. Therefore, in the future, the impact of urbanization on the trends in temperature series needs to be evaluated and eliminated from existing homogenized data. Urbanization bias-adjusted data series will be better able to represent the real changes in background temperature. This is an important and urgent issue to be solved in the future.

5. CONCLUSIONS

We established an extended set of monthly mean SAT data series in China going back to the late 19th century through consistent quality control, interpolation, and homogenization. The dataset includes 57 stations for monthly mean temperature and 50 stations for monthly mean maximum and minimum temperatures. Early-year data recovered and digitized by ACRE China were used to supplement the station observations in the new dataset.

RHtest homogenization methods were applied to adjust the major inhomogeneous biases in the original data. In comparison with the raw data, the adjusted data series of annual mean SATs indicates more significant warming. The warming trends of the original and adjusted series of annual mean SAT are 0.13 and 0.14°C per decade, respectively, during 1901–2020.

The regional series of annual mean SATs for China during 1951–2020 constructed from the 57 stations is quite consistent with that calculated from a denser network of stations. The linear trend of the regional series of annual mean SATs for 1901–2020 is large and significant, with a more obvious warming of 0.07°C per decade for the period of 1951–2020.

The trends of the annual mean maximum and minimum temperature series for China based on the new dataset are comparable to those based on other currently available datasets. The large and significant decline in the DTR in North, Northeast, and Northwest China is mostly due to the more rapid increase in minimum temperature than in maximum temperature.

Uncertainty in the trend estimates of annual mean temperature, maximum temperature, minimum temperature, and DTR is mainly caused by the relatively sparse distribution of stations before 1950. There is a need to strengthen the recovery and digitization of the early 20th century data in the coming years. Another big issue related to the uncertainty of the trend estimates is the effect of urbanization on the regional long-term temperature series. This should be further investigated in the future.

Acknowledgements. This study was supported by the National Key Research and Development Project (Grant No. 2018YFA0605603). Martha Evonuk PhD from Liwen Bianji (Edanz) (www.liwenbianji.cn/) edited the English text of a draft of the manuscript.

LITERATURE CITED

Bayazit M, Onoz B (2007) To prewhiten or not to prewhiten in trend analysis. Hydrol Sci J 52:611–624

Bian T, Ren G, Yue Y (2017) Effect of urbanization on land-surface temperature at an urban climate station in North China. Boundary-Layer Meteorol 165:553–567

Cao L, Yan Z (2012) Progress in research on homogenization of climate data. Adv Clim Chang Res 3:59–67

Cao LJ, Zhao P, Yan ZW, Jones PD, Zhu YN, Yu Y, Tang GL (2013) Instrumental temperature series in eastern and central China back to the nineteenth century. J Geophys Res Atmos 118:8197–8209

Cao LJ, Yan ZW, Zhao P, Zhu YN and others (2017) Climatic warming in China during 1901–2015 based on an extended dataset of instrumental temperature records. Environ Res Lett 12:064005

Cerveny RS, Lawrimore J, Edwards R, Landsea C (2007) Extreme weather records: compilation, adjudication, and publication. Bull Am Meteorol Soc 88:853–860

Chen T, Chen X (2007) Variation of diurnal temperature range in China in the past 50 years. Plateau Meteorol 26: 150–157

Ding Y, Liu Y, Liang S, Ma X and others (2014) Interdecadal variability of the East Asian Winter Monsoon and its possible links to global climate change. J Meteorol Res 28: 693–713

Dong D, Huang G (2015) Relationship between altitude and variation characteristics of the maximum temperature, minimum temperature, and diurnal temperature range in China. Chin J Atmos Sci 39:1011–1024 (in Chinese)

Easterling DR, Horton B, Jones PD, Peterson TC and others (1997) Maximum and minimum temperature trends for the globe. Science 277:364–367

Easterling DR, Peterson TC (1995) A new method for detecting and adjusting for undocumented discontinuities in climatological time series. Int J Climatol 15:369–377

Easterling D, Evans J, Groisman P, Karl T, Kunel K, Ambenje P (2000) Observed variability and trends in extreme climate events: a brief review. Bull Am Meteorol Soc 81:417–426

Harris I, Osborn TJ, Jones P, Lister D (2020) Version 4 of the CRU TS monthly high-resolution gridded multivariate climate dataset. Sci Data 7:109

Hua L, Ma Z, Zeng Z (2006) The comparative analysis of the changes of extreme temperature and extreme diurnal temperature range of large cities and small towns in eastern China. Chin J Atmos Sci 30:80–92 (in Chinese)

IPCC (2013) Climate change 2013: the physical science basis. Contribution of Working Group I to the fifth assessment report of the Intergovernmental Panel on Climate Change. Cambridge University Press, Cambridge

IPCC (2021) Climate change 2021: the physical science basis. Contribution of Working Group I to the sixth assessment report of the Intergovernmental Panel on Climate Change. Cambridge University Press, Cambridge, p 3–32

Jones PD (2016) The reliability of global and hemispheric surface temperature records. Adv Atmos Sci 33:269–282

Jones PD, Hulme M (1996) Calculating regional climatic time series for temperature and precipitation: methods and illustrations. Int J Climatol 16:361–377

Karl TR, Jones PD, Knight RW, Kukla G and others (1993) A new perspective on recent global warming: asymmetric trends of daily maximum and minimum temperature. Bull Am Meteorol Soc 74:1007–1024

Karl TR, Kukla G, Razuvayev VN, Changery MJ and others (1991) Global warming: evidence for asymmetric diurnal temperature change. Geophys Res Lett 18:2253–2256

Kendall MG (1975) Rank correlation measures. Charles Griffin, London

Li J, Ren GY, Ren YY, Zhang L (2014) Effect of data homogenization on temperature trend estimation and urban bias at Shenyang station. Daqi Kexue Xuebao 37:297–303 (in Chinese)

Li Q, Yang Y (2019) Comments on 'Comparing the current and early 20th century warm periods in China' by Soon W., R. Connolly, M. Connolly et al. Earth-Sci Rev 198: 102886

Li QX, Dong WJ, Li W, Gao XR, Jones P, Kennedy J, Parker D (2010) Assessment of the uncertainties in temperature change in China during the last century. Chin Sci Bull 55:1974–1982

Li Q, Zhang L, Xu W, Zhou T, Wang J, Zhai P, Jones P (2017) Comparisons of time series of annual mean surface air temperature for China since the 1900s: observations, model simulations, and extended reanalysis. Bull Am Meteorol Soc 98:699–711

Li Z, Yan Z, Cao L, Jones P (2014) Adjusting inhomogeneous daily temperature variability using wavelet analysis. Int J Climatol 34:1196–1207

Liu B, Xu M, Henderson M, Qi Y, Li Y (2004) Taking China's temperature: daily range, warming trends, and regional variations, 1955–2000. J Clim 17:4453–4462

Mann HB (1945) Non-parametric tests against trend. Econometrica 13:245–259

NMIC (National Meteorological Information Center) (2013a) Assessment report of homogenized monthly temperature data set of national surface meteorological stations in China (V1.0). National Meteorological Information Center, Beijing (in Chinese)

NMIC (2013b) Assessment report of homogenized daily temperature data set of national surface meteorological stations in China (V1.0). National Meteorological Information Center, Beijing (in Chinese)

Osborn TJ, Jones PD, Lister DH, Morice CP and others (2021) Land surface air temperature variations across the globe updated to 2019: the CRUTEM5 dataset. J Geophys Res Atmos 126:e2019JD032352

Qin DH, Chen ZL, Luo Y (2007) Updated understanding of climate change sciences. Adv Clim Chang Res 3:63–73 (in Chinese)

Ren GY, Li J, Ren YY, Chu ZY and others (2015) An integrated procedure to determine a reference station network for evaluating and adjusting urban bias in surface air temperature data. J Appl Meteorol Climatol 54: 1248–1266

Ren G, Zhan Y, Ren Y, Wen K and others (2023) Observed changes in temperature and precipitation over Asia, 1901–2020. Clim Res 90:31–43

Ren Y, Ren G (2011) A remote-sensing method of selecting reference stations for evaluating urbanization effect on surface air temperature trends. J Clim 24:3179–3189

Ren YY, Ren GY, Sun XB, Shrestha AB and others (2017) Observed changes in surface air temperature and precipitation in the Hindu Kush Himalayan region over the last 100-plus years. Adv Clim Chang Res 8:148–156

Sen PK (1968) Estimates of the regression coefficient based on Kendall's tau. J Am Stat Assoc 63:1379–1389

Shen D, Varis O (2001) Climate change in China. Ambio 30: 381–383

Soon W, Connolly R, Connolly M (2015) Re-evaluating the role of solar variability on Northern Hemisphere temperature trends since the 19th century. Earth Sci Rev 150: 409–452

Soon W, Connolly R, Connolly M, O'Neill P and others (2018) Comparing the current and early 20th century warm periods in China. Earth Sci Rev 185:80–101

Sun X, Ren G, Xu W, Li Q, Ren Y (2017) Global land-surface air temperature change based on the new CMA GLSAT data set. Sci Bull (Beijing) 62:236–238

Sun X, Ren G, Ren Y, Fang Y and others (2018) A remarkable climate warming hiatus over Northeast China since 1998. Theor Appl Climatol 133:579–594

Sun X, Ren G, You Q, Ren Y and others (2019) Global diurnal temperature range (DTR) changes since 1901. Clim Dyn 52:3343–3356

Sun XB, Wang CZ, Ren GY (2021) Changes of diurnal temperature range over East Asia from 1901 to 2018 and its relationship with precipitation. Clim Change 166:44

Tang G, Ren G (2005) Reanalysis of surface air temperature change of the last 100 years over China. Climatic Environ Res 10:791–798 (in Chinese)

Tang G, Ding Y, Wang S, Ren G and others (2009) Comparative analysis of the time series of surface air temperature over China for the last 100 years. Adv Clim Chang Res 5:71–78 (in Chinese)

Tang H, Zhai P, Wang Z (2005) On change in mean maximum temperature, minimum temperature and diurnal range in China during 1951–2002. Climatic Environ Res 10:728–735 (in Chinese)

Theil H (1992) A rank-invariant method of linear and polynomial regression analysis. In: Raj B, Koerts J (eds) Henri Theil's contributions to economics and econometrics.

Advanced Studies in Theoretical and Applied Econometrics, Vol 23. Springer, Dordrecht, p 345–381

Trenberth KE, Fasullo JT (2013) An apparent hiatus in global warming? Earth's Future 1:19–32

Wang D, Hou Y, He J, Luan J (2014) Responses of temperature in different regions and seasons to the reduction of global warming. The 31st Annual Meeting of the Chinese Meteorological Society: S15 Subtropical Meteorology and Ecological Environment Impact (in Chinese)

Wang H, Li J, Gao Z, Yim S and others (2019) High-spatial-resolution population exposure to $PM_{2.5}$ pollution based on multi-satellite retrievals: a case study of seasonal variation in the Yangtze River Delta, China in 2013. Remote Sens 11:2724

Wang SW (2001) Advances in modern climatology research. Meteorological Press, Beijing (in Chinese)

Wang SW, Ye JL (1995) An analysis of global warming during the last one hundred years. Chin J Atmos Sci 19: 545–553 (in Chinese)

Wang SW, Ye JL, Gong DY, Zhu JH and others (1998) Construction of mean annual temperature series for the last one hundred years in China. Yingyong Qixiang Xuebao 9:392–401 (in Chinese)

Wang S, Zhu J, Cai J (2004) Interdecadal variability of temperature and precipitation in China since 1880. Adv Atmos Sci 21:307–313

Wang XL (2007) Penalized maximal *t*-test for detecting undocumented mean change in climate data series. J Appl Meteorol Climatol 46:916–931

Wang XL (2008a) Accounting for autocorrelation in detecting mean shifts in climate data 493 series using the penalized maximal *t* or *F* Test. J Appl Meteorol Climatol 47:2423–2444

Wang XL (2008b) Penalized maximal *F* test for detecting undocumented mean shift without trend change. J Atmos Ocean Technol 25:368–384

Wang XL, Feng Y (2010) RHtestsV3 user manual. Climate Research Division, Science and Technology Branch, Environment Canada, Toronto

Wen KM (2020) Study on the correction of urbanization bias in surface air temperature records in China. PhD thesis, China University of Geosciences, Wuhan (in Chinese)

Wen K, Ren G, Li J, Zhang A, Ren Y, Sun X, Zhou Y (2019) Recent surface air temperature change over mainland China based on an urbanization-bias adjusted dataset. J Clim 32:2691–2705

Xu X, Du YG, Tang JP, Wang Y (2011) Variations of temperature and precipitation extremes in recent two decades over China. Atmos Res 101:143–154

Xue W, Guo J, Zhang Y, Zhou S and others (2019) Declining diurnal temperature range in the North China Plain related to environmental changes. Clim Dyn 52: 6109–6119

Yang J, Liu H, Ou CQ, Lin G and others (2013) Global climate change: impact of diurnal temperature range on mortality in Guangzhou, China. Environ Pollut 175:131–136

Yang X, Leung LR, Zhao N, Zhao C and others (2017) Contribution of urbanization to the increase of extreme heat events in an urban agglomeration in east China. Geophys Res Lett 44:6940–6950

Yang Y, Wu B, Shi C, Zhang J and others (2013) Impacts of urbanization and station-relocation on surface air temperature series in Anhui Province, China. Pure Appl Geophys 170:1969–1984

Yang Y, Zhang MY, Li QX, and others (2020) Modulations of surface thermal environment and agricultural activity on intraseasonal variations of summer diurnal temperature range in the Yangtze River Delta of China. Sci Total Environ 736:139445

Yang Y, Guo M, Ren G, Liu S and others (2022) Modulation of wintertime canopy urban heat island (CUHI) intensity in Beijing by synoptic weather pattern in planetary boundary layer. J Geophys Res Atmos 127: e2021JD035988

Zhai PM, Ren FM (1997) On changes of China's maximum and minimum temperature in the recent 40 years. Acta Meteorol Sin 55:418–429 (in Chinese)

Zhang L, Ren GY, Ren YY, Zhang AY, Chu ZY, Zhou YQ (2014) Effect of data homogenization on estimate of temperature trend: a case of Huairou station in Beijing Municipality. Theor Appl Climatol 115:365–373

Zhang Y (2014) Evaluation and correction of urbanization bias in surface temperature records over eastern China in the last 100 years. Chinese Academy of Meteorological Sciences, Beijing

Zhao P, Jones P, Cao L, Yan Z and others (2014) Trend of surface air temperature in eastern China and associated large-scale climate variability over the last 100 years. J Clim 27:4693–4703

Zhou Y, Ren G (2011) Change in extreme temperature event frequency over mainland China, 1961–2008. Clim Res 50:125–139

Editorial responsibility: Eduardo Zorita, Geesthacht, Germany
Reviewed by: 3 anonymous referees

Submitted: September 5, 2022
Accepted: June 16, 2023
Proofs received from author(s): August 14, 2023